Marine Geology 341 (2013) 46–57

Contents lists available at SciVerse ScienceDirect

Marine Geology

journal homepage: www.elsevier.com/locate/margeo

A submarine canyon as a climate archive — Interaction of the Antarctic Intermediate Water with the Mar del Plata Canyon (Southwest Atlantic)

Ines Voigt [a,*], Ruediger Henrich [b], Benedict M. Preu [a,1], Alberto R. Piola [c,d], Till J.J. Hanebuth [a], Tilmann Schwenk [b], Cristiano M. Chiessi [e]

[a] MARUM — Center for Marine Environmental Sciences, University of Bremen, D-28203 Bremen, Germany
[b] MARUM — Center for Marine Environmental Sciences and Faculty of Geosciences, University of Bremen, Germany
[c] Servicio de Hidrografia Naval (SHN), Buenos Aires, Argentina
[d] Dept. Ciencias de la Atmósfera y los Océanos, FCEN, Universidad de Buenos Aires and Instituto Franco-Argentino sobre, Estudios de Clima y sus Impactos, CNRS/CONICET, Argentina
[e] School of Arts, Sciences and Humanities, University of São Paulo, Brazil

ARTICLE INFO

Article history:
Received 26 October 2012
Received in revised form 6 May 2013
Accepted 8 May 2013
Available online 18 May 2013

Communicated by D.J.W. Piper

Keywords:
Southwest Atlantic
Antarctic Intermediate Water
Drift deposition
Submarine Canyon
El Niño/Southern Oscillation (ENSO)

ABSTRACT

The Mar del Plata Canyon is located at the continental margin off northern Argentina in a key intermediate and deep-water oceanographic setting. In this region, strong contour currents shape the continental margin by eroding, transporting and depositing sediments. These currents generate various depositional and erosive features which together are described as a Contourite Depositional System (CDS). The Mar del Plata Canyon intersects the CDS, and does not have any obvious connection to the shelf or to an onshore sediment source. Here we present the sedimentary processes that act in the canyon and show that continuous Holocene sedimentation is related to intermediate-water current activity. The Holocene deposits in the canyon are strongly bioturbated and consist mainly of the terrigenous "sortable silt" fraction (10–63 μm) without primary structures, similarly to drift deposits. We propose that the Mar del Plata Canyon interacts with an intermediate-depth nepheloid layer generated by the northward-flowing Antarctic Intermediate Water (AAIW). This interaction results in rapid and continuous deposition of coarse silt sediments inside the canyon with an average sedimentation rate of 160 cm/kyr during the Holocene. We conclude that the presence of the Mar del Plata Canyon decreases the transport capacity of AAIW, in particular of its deepest portion that is associated with the nepheloid layer, which in turn generates a change in the contourite deposition pattern around the canyon. Since sedimentation processes in the Mar del Plata Canyon indicate a response to changes of AAIW contour-current strength related to Late Glacial/Holocene variability, the sediments deposited within the canyon are a great climate archive for paleoceanographic reconstructions. Moreover, an additional involvement of (hemi) pelagic sediments indicates episodic productivity events in response to changes in upper ocean circulation possibly associated with Holocene changes in intensity of El Niño/Southern Oscillation.

1. Introduction

Submarine canyons are common morphological features at continental margins worldwide (Harris and Whiteway, 2011). They are important natural conduits for the transfer of terrigenous sediments to the deep sea, but also represent considerable (temporary) sinks for enhanced accumulation of modern sediments (Carson et al., 1986). The traditional approach of submarine canyons implies that sediment discharged by a nearby river system and/or by sediment movement across the continental shelf is carried down the canyon by gravitational processes and is deposited as turbidites. However, as most of the world's canyons (Harris and Whiteway, 2011), the Mar del Plata Canyon at the continental margin off northern Argentina does not have any obvious connection to the shelf or an onshore river system (e.g., La Plata River) (Krastel et al., 2011), and is therefore isolated from shelf-originated down-slope processes. The canyon is incorporated into a significant Contourite Depositional System (CDS) extensively present at the continental margin off northern Argentina, whose sedimentation processes are primarily controlled by northward-flowing Antarctic water masses, in particular by the Antarctic Intermediate Water (AAIW) (Hernández-Molina et al.,

* Corresponding author at: MARUM - Center for Marine Environmental Sciences and Faculty of Geosciences, University of Bremen, Klagenfurter Str., D-28203 Bremen, Germany. Tel.: +49 421 218 65204; fax: +49 421 218 65219.
E-mail addresses: ines.voigt@uni-bremen.de (I. Voigt), henrich@uni-bremen.de (R. Henrich), bpreu@uni-bremen.de, bpreu@chevron.com (B.M. Preu), apiola@hidro.gov.ar (A.R. Piola), thanebuth@uni-bremen.de (T.J.J. Hanebuth), tschwenk@uni-bremen.de (T. Schwenk), chiessi@usp.br (C.M. Chiessi).
[1] Now at Chevron Upstream Europe, Chevron North Sea Limited, Aberdeen AB15 6XL, United Kingdom.

0025-3227/$ – see front matter © 2013 Elsevier B.V. All rights reserved.
http://dx.doi.org/10.1016/j.margeo.2013.05.002

2009; Preu et al., 2013) (Fig. 1). Drift deposits (typical deposits formed within CDSs) have been comprehensively described from (sub)-recent deposits throughout the world's deep ocean environments (Stow and Lovell, 1979; Stow et al., 2002; Rebesco et al., 2008), whereas submarine canyons incorporated into CDSs have not long been perceived (Marchès et al., 2007; Lastras et al., 2011). Although recent studies propose that submarine canyons significantly alter the hydrodynamics of contour currents, thereby leading to significant changes in contourite drift construction (Marchès et al., 2007); the sedimentary processes in these submarine canyons remain poorly understood.

Here we investigate the Holocene sedimentary records from the Mar del Plata Canyon, and consider the sedimentary processes and sediment characteristics of a submarine canyon that intersects a CDS. The deposits in the Mar del Plata Canyon yield insights into the interaction of the submarine canyon with an intermediate nepheloid layer (INL) generated by the AAIW, as well as into the role of the Mar del Plata Canyon as a considerable (temporary) sink for Late Glacial/Holocene sediments.

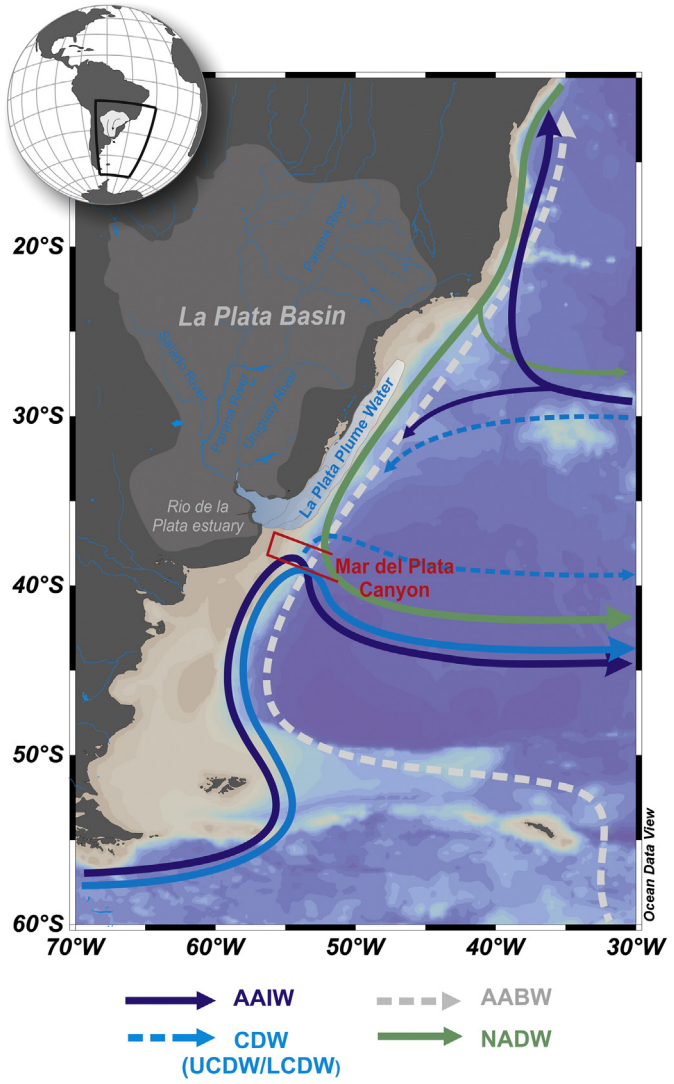

Fig. 1. Schematic intermediate and deep-water circulation in the Southwest Atlantic after Stramma and England (1999). Different water masses formed in remote areas of the world extend into that area and generate a highly complex vertical stratification structure. In the deep ocean, this structure is dominated by contributions from intermediate- and deep water masses, including (from top to bottom) the Antarctic Intermediate Water (AAIW), the Upper Circumpolar Deep Water (UCDW), the North Atlantic Deep Water (NADW), the Lower Circumpolar Deep Water (LCDW) and the Antarctic Bottom Water (AABW). The La Plata River discharges into the ocean waters from La Plata basin covering a large area of South America.

In highly energetic regions such as the Southwest Atlantic the sedimentary records found in submarine canyons may thus provide high temporal-resolution climate archives which can be used for paleoclimate and/or paleoceanographic reconstructions.

2. Regional setting

The Southwest Atlantic is a key location in the global intermediate and deep-water circulation (Fig. 1). Different water masses formed in remote areas of the world extend into that area and generate a highly complex vertical stratification structure. In the upper ocean, this structure is dominated by the encounter of southward flowing Brazil Current and northward-flowing Malvinas- (Falkland) Current generating one of the most energetic regions of the world ocean; the Brazil–Malvinas Confluence (BMC) (Chelton et al., 1990; Peterson and Stramma, 1991; Piola and Matano, 2001). In the deep ocean, the vertical stratification structure is dominated by contributions from intermediate- and deep water masses including (from top to bottom) the Antarctic Intermediate Water (AAIW, ~500–1000 m), the Circumpolar Deep Water (CDW, ~1000–4000 m) and the Antarctic Bottom Water (AABW, >4000 m) (Reid and Patzert, 1977; Stramma and England, 1999) (Figs. 1 & 2B). By penetrating into the CDW, the North Atlantic Deep Water (NADW, 2000–3000 m) vertically divides this water mass into two layers: the upper CDW (UCDW) and the lower CDW (LCDW). These contour-following bottom currents are able to significantly shape the continental margin by eroding, transporting and depositing sediments at the sea floor (Stow et al., 2002, 2008; Rebesco et al., 2008). Along the Argentine margin they generate various depositional (drifts) and erosional features (terraces) which together form a Contourite Depositional System (CDS) (Hernández-Molina et al., 2009).

The Mar del Plata Canyon, a relatively straight, deeply incised bathymetric feature, is incorporated into this CDS at around 38°S (Krastel et al., 2011) (Figs. 1 & 2B). The whole canyon is confined to the continental slope forming a so-called “blind” canyon (Harris and Whiteway, 2011) that does not have any obvious connection to the shelf or to modern terrestrial fluvial systems (e.g., La Plata River) (Krastel et al., 2011). The Mar del Plata Canyon head is situated on the upper continental slope at a water depth of ~1000 m and extends for ~110 km downslope to a water depth of ~3900 m. Mapping between the shelf break and the canyon by hydroacoustic and seismic methods shows neither any incision at the modern seafloor nor a refilled or sediment buried upslope continuation of the Mar del Plata Canyon (Krastel et al., 2011). The upper part of the Mar del Plata Canyon incises the Ewing contourite terrace, a pronounced bathymetric feature along the northern Argentine continental slope (Krastel et al., 2011).

Contourite terraces at the depth of ~1000 m are observed along the entire continental margin off Argentina, and have been developed in depositional and erosive phases over time caused by the interaction of northward-flowing AAIW and UCDW (Hernández-Molina et al., 2009, 2010; Lastras et al., 2011). At present, turbulent processes at the lower boundary of the AAIW inhibit sediment deposition over large areas on the Ewing terrace (Preu et al., 2013) (Fig. 2B). The hypothesis of strong AAIW in the study area is also supported by the OCCAM Global Ocean Model (Gwilliam, 1996) indicating flow velocities of ~15–20 cm/s at 1000 m water depth.

Measurements of high turbidity which are part of the world ocean nepheloid layer composition data base assembled by the Lamont–Doherty Earth Observatory (Fig. 2A) indicate a very pronounced intermediate nepheloid layer (INL) testifying to strong current activity in the depth range of AAIW. Nepheloid layers contain significant amounts of suspended sediment, and therefore have been inferred to play an important role in the formation of drift deposits (Rebesco et al., 2008). The amount of suspended sediments decreases drastically toward the UCDW, and indicates the lower transport capacity of the UCDW. Accordingly, directly beneath the high velocity core of the AAIW, toward

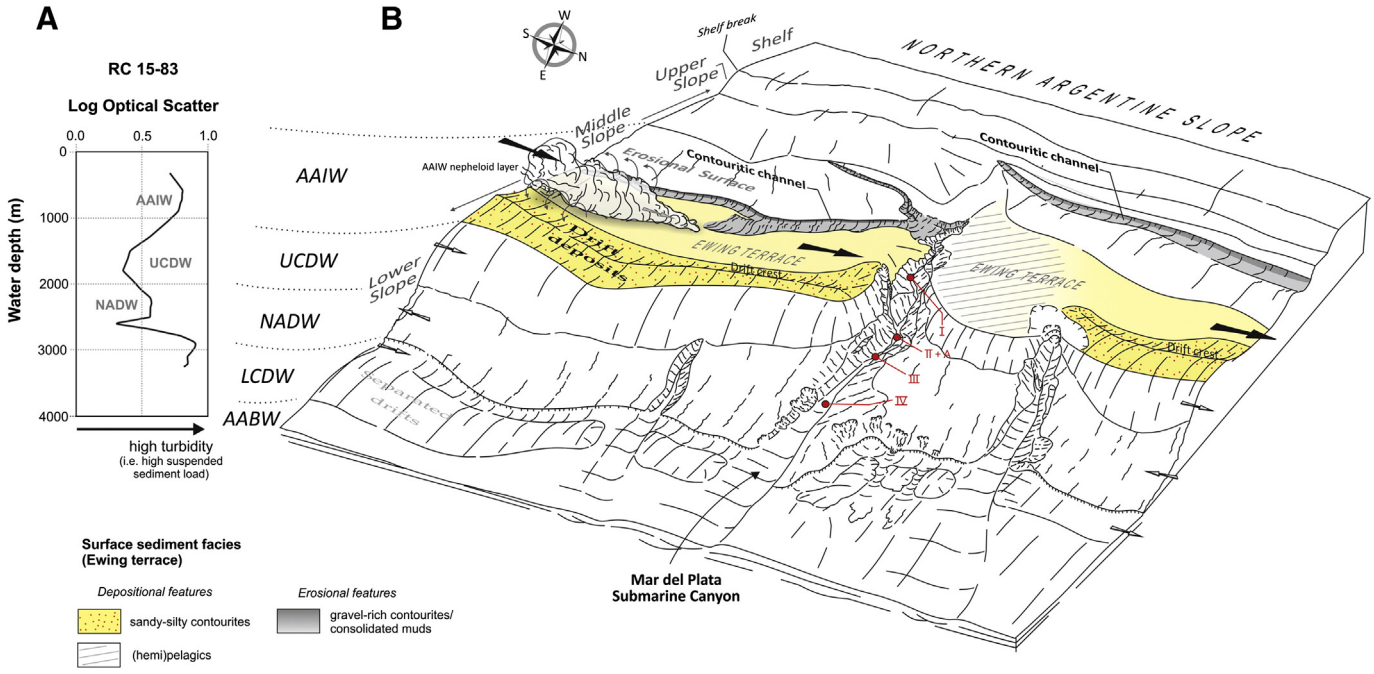

Fig. 2. (A) Measurements of high turbidity at the southern flank of the Mar del Plata Canyon suggest a very pronounced intermediate nepheloid layer testifying to strong current activity in the depth range of AAIW. (B) Morpho-sedimentary map of the NE Argentine margin after Preu et al. (2013) shows that the Mar del Plata Canyon is incorporated into a Contourite Depositional System. Yellow-colored surfaces indicate the Ewing terrace that is located at the lower boundary of the AAIW. Surface sediment facies along the Ewing terrace after Bozzano et al. (2011). Erosion/non-deposition takes place at the inner part of the Ewing terrace while drift deposition takes place at the outer part of the terrace. Drift deposits occur south of the Mar del Plata Canyon, but are missing directly north of it. Sediment cores: I — GeoB13832-2, II — GeoB13833-2, III — GeoB13862-1, IV — GeoB13861-1 (for more information about the sediment cores see Table. 1). CTD station: A — GeoB13833-3. AAIW — Antarctic Intermediate Water; UCDW — Upper Circumpolar Deep Water; NADW — North Atlantic Deep Water; LCDW — Lower Circumpolar Deep Water; AABW — Antarctic Bottom Water. (For interpretation of the references to color in this figure legend, the reader is referred to the web version of this article.)

the interface of AAIW/UCDW, sediment material accumulates from the suspension of the nepheloid layer and leads to the formation of drift deposits on the Ewing terrace (Preu et al., 2013) (Fig. 2A, B). Drift deposits on the outer parts of the Ewing terrace are thus primarily influenced by sediments transported by the AAIW, particularly by its deepest portion associated with the nepheloid layer. A marked change in contourite drift construction occurs around the Mar del Plata Canyon. Drift deposits are present south of the canyon, but are missing directly north of it (Fig. 2B).

The La Plata basin covers about 3.6 million km^2 thus being the second largest drainage basin in South America. It drains nearly 20% of the surface area of South America and discharges about 23,000 m^3 s^{-1} of freshwater on the Southwest Atlantic shelf (Mechoso et al., 2001) (Fig. 1). The La Plata derived waters influence nutrient distribution and, as a consequence, phytoplankton production of the adjacent coastal waters (Ciotti et al., 1995). Accordingly, primary production on the Southwest Atlantic shelf at 35°S is largely enhanced by fertilization from the La Plata River discharge (Hubold, 1980a, 1980b; Carreto et al., 1995). Recent studies indicate that on the annual mean the present-day La Plata plume is directed northwards (Piola et al., 2000) (Fig. 1). Thereby, the plume distribution sets the sediment distribution off the Rio del la Plata estuary, where fluviomarine facies have been traced on the Uruguayan middle shelf (e.g., along the northern river margin) (Urien and Ewing, 1974). However, the La Plata plume undergoes large interannual variations related to El Niño/Southern Oscillation (ENSO) (Piola et al., 2005, 2008). In particular the effects of wind anomalies during strong El Niño events prevent an along-shore northward spreading of the La Plata plume and force the water masses offshore in the general direction to the Mar del Plata Canyon. This variability also impacts the primary production in the upper water column as recorded in SeaWiFS-derived chlorophyll anomalies (Ciotti et al., 1995; Garcia and Garcia, 2008), which suggest the offshore extension of La Plata plume waters during strong El Niño events.

3. Material & methods

This study is based on the stratigraphic, sedimentological and geochemical analyses of four gravity cores (i.e., GeoB13832-2, GeoB13833-2, GeoB13862-1 and GeoB13861-1) recovered from the thalweg of the Mar del Plata Canyon (Fig. 2B, Table 1). The cores were collected during research cruise M78/3a,b with the German RV METEOR (Krastel and Wefer, 2012).

3.1. Stratigraphy

Dating of the sedimentary sequences was performed by using AMS-^{14}C measurements on 12 samples of planktonic foraminifera *Globorotalia inflata* (>150 μm fraction) (Table 2, Poznan Radiocarbon Laboratory, Poland). Foraminiferal radiocarbon ages are assumed as the most reliable source of information about the time of sediment deposition since these tests are less susceptible to lateral transport due to their large grain-size (Fok-Pun and Komar, 1983; Ohkouchi et al., 2002; Mollenhauer et al., 2006). The radiocarbon dates were calibrated with the CALIB 6.0 radiocarbon calibration program (Stuiver and Reimer, 1993) by applying the Marine09 calibration

Table 1
Location of sediment cores used in this study.

Cruise	Core	Latitude	Longitude	Water depth (m)	Recovery (cm)
M78/3a	GeoB13832-2	37°90.23′ S	54°14.12′ W	2205	556
M78/3a	GeoB13833-2	37°95.20′ S	53°83.68′ W	3405	796
M78/3b	GeoB13862-1	38°01.85′ S	53°74.50′ W	3588	1016
M78/3b	GeoB13861-1	38°09.18′ S	53°60.98′ W	3715	668

Table 2
Accelerator mass spectrometry (AMS) radiocarbon dates and calibrated ages.

Sample code	Depth (cm)	Species	Radiocarbon age ± 1σ error (a B.P.)	Calibrated age, interpolated from 2σ range (cal ka B.P.)	2σ calibrated age range (cal ka B.P.)
Core GeoB13862-1					
Poz-38071	143	*G. inflata*	1790 ± 140	1.36	1.05–1.67
Poz-42354	258	*G. inflata*	4000 ± 50	4.00	3.85–4.15
Poz-38072	393	*G. inflata*	5380 ± 60	5.75	5.61–5.89
Poz-42355	490	*G. inflata*	5840 ± 80	6.25	6.06–6.43
Poz-42356	556	*G. inflata*	6140 ± 50	6.57	6.44–6.70
Poz-38074	669	*G. inflata*	8530 ± 70	9.18	8.99–9.36
Poz-38075	793	*G. inflata*	9740 ± 70	10.64	10.46–10.83
Poz-38076	913	*G. inflata*	10020 ± 130	10.91	10.61–11.22
Poz-42353	1007	Mixed planktonic foraminifera[a]	11210 ± 60	12.72	12.58–12.86
Core GeoB13832-2					
Poz-36053	50	*G. inflata*	1335 ± 35	0.87	0.78–0.95
Poz-36055	535	*G. inflata*	4750 ± 50	5.03	4.85–5.20
Core GeoB13833-2					
Poz-42357	777	*G. inflata*	5910 ± 50	6.33	6.22–6.43

[a] Mixed planktonic foraminifera contained *G. inflata*, *G. bulloides* and *N. pachyderma*.

curve (Reimer et al., 2009) and no ΔR. All ages are given in calibrated thousands of years before present (ka B.P.). Stratigraphic correlation between the four sediment cores was based on ^{14}C ages and X-ray fluorescence (XRF) down-core records of Ca and Fe (Fig. 3).

3.2. X-radiographs and grain-size analysis

The sedimentary facies from each core were characterized by visual core descriptions and X-radiographs. Bulk and terrigenous grain-size distributions for GeoB13832-2, GeoB13833-2 and GeoB13862-1 were measured with a Coulter Laser Particle Sizer LS200. In order to isolate the terrigenous fraction (i.e., opal-, organic carbon- and carbonate-free) from the marine sediments, several pretreatment steps were undertaken to remove biogenic constituents (for methods see Mulitza et al., 2008).

3.3. Bulk geochemistry

Samples for bulk geochemical analyses were freeze dried and pulverized in an agate mortar. For the determination of organic carbon, calcium carbonate was removed by repeatedly adding aliquots of 0.25 N HCl. Total carbon (TC) and total organic carbon (TOC) were measured in homogenized sub-samples of bulk sediments, using a LECO CS-300 element analyzer. Carbonate was calculated from the difference between TC and TOC, and expressed as calcite [$CaCO_3 = (TC - TOC) * 8.33$]. Opal content was determined by the sequential leaching technique by DeMaster (1981) with modifications by Müller and Schneider (1993).

3.4. X-ray fluorescence (XRF scanning)

The XRF scanner is a nondestructive method for high resolution and relatively fast analyses of major and minor elements by scanning split sediment cores (Jansen et al., 1998). XRF scans were performed with an AVAATECH XRF core scanner at MARUM, University of Bremen.

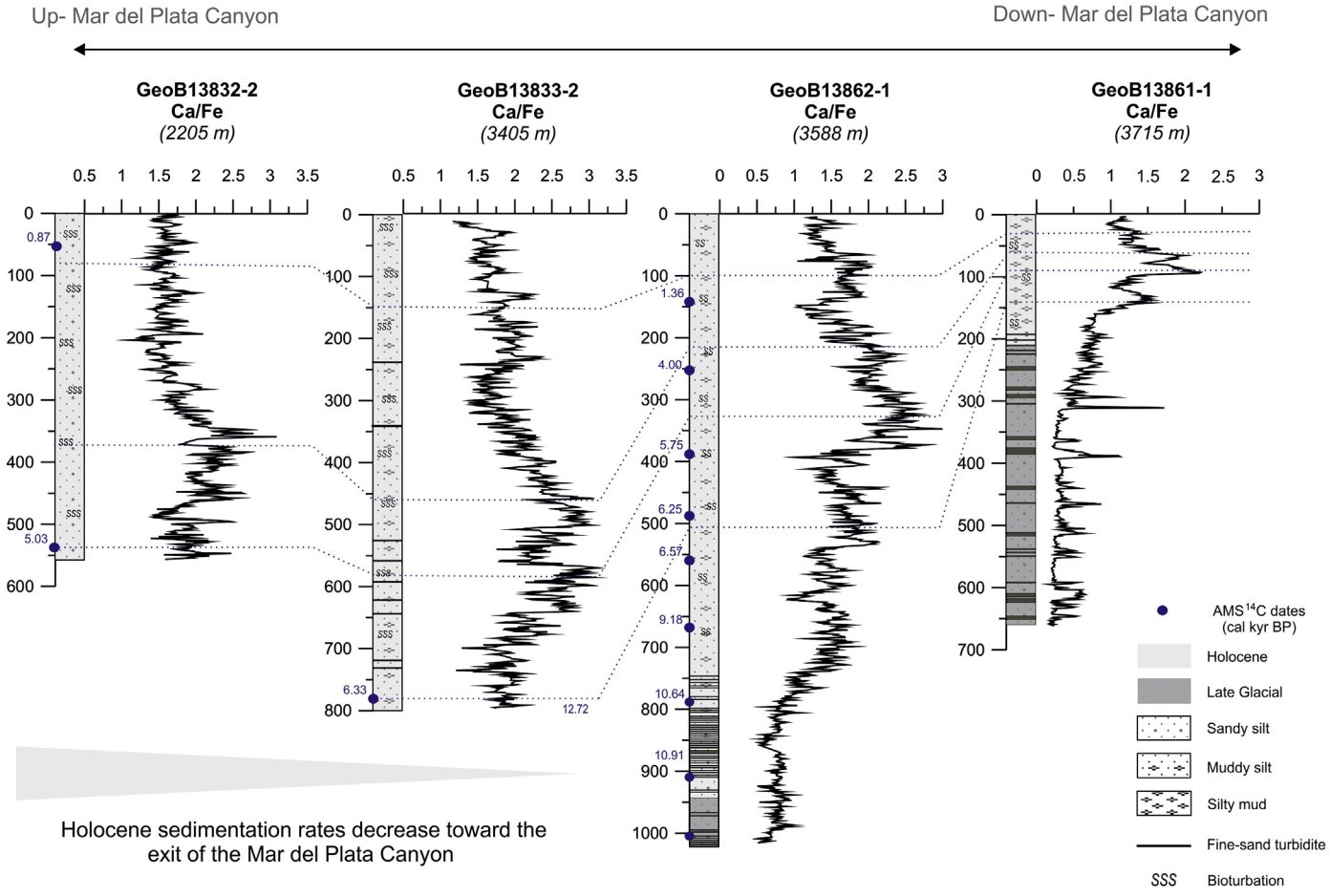

Fig. 3. Stratigraphic correlation between the sediment cores recovered in the Mar del Plata Canyon. The correlation is based on both calibrated AMS-^{14}C ages and down-core Ca/Fe records. The highest average sedimentation rate is observed in GeoB13832-2 (190 cm/kyr), followed by GeoB13833-2 (170 cm/kyr), and GeoB13862-1 (140 cm/kyr). The thickest Holocene deposits appear to be concentrated in the upper part of the canyon.

Element intensities, given as counts per second (cps), were measured on the split cores at 1-cm intervals. Prior and after analysis, the instrument was calibrated against a set of pressed powder standards. From the whole set of elements measured, we show here Ca/Fe and Si/Al. Calcium and Fe relative fluctuations trace the relative abundance of biogenic carbonate and terrigenous material, respectively (Govin et al., 2012). Relative changes in Si and Al typically reflect changes in the input of biogenic opal or the strength of continental weathering.

3.5. CTD

A CTD cast was performed during the R/V Meteor cruise M78/3a,b in the central part of the Mar del Plata Canyon at site GeoB13833-3. Additionally, an along-slope salinity and dissolved oxygen section in the vicinity of the Mar del Plata Canyon was constructed based on 36 historical hydrographic stations occupied on a relatively narrow strip between 37 and 39°S roughly following the 1300–2000 m isobath range.

4. Results

4.1. Holocene: Homogeneous coarse-silt sedimentary facies

All cores reveal remarkably high and almost continuous sedimentation rates during the Holocene (Fig. 3). The highest average sedimentation rate is observed in GeoB13832-2 (~190 cm/kyr), followed by GeoB13833-2 (~170 cm/kyr), and GeoB13862-1 (~140 cm/kyr). Since sedimentation rates decrease toward the exit of the canyon, the thickest Holocene deposits appear to be concentrated in the upper part of the canyon (Fig. 3).

4.1.1. Sedimentary structures and characteristics

The typical sedimentary structures and characteristics of the Holocene facies are shown in Fig. 4 for GeoB13862-1. Accordingly, the Holocene sequence is defined by a coarse-silt dominated facies without any primary sedimentary structures. The most characteristic feature

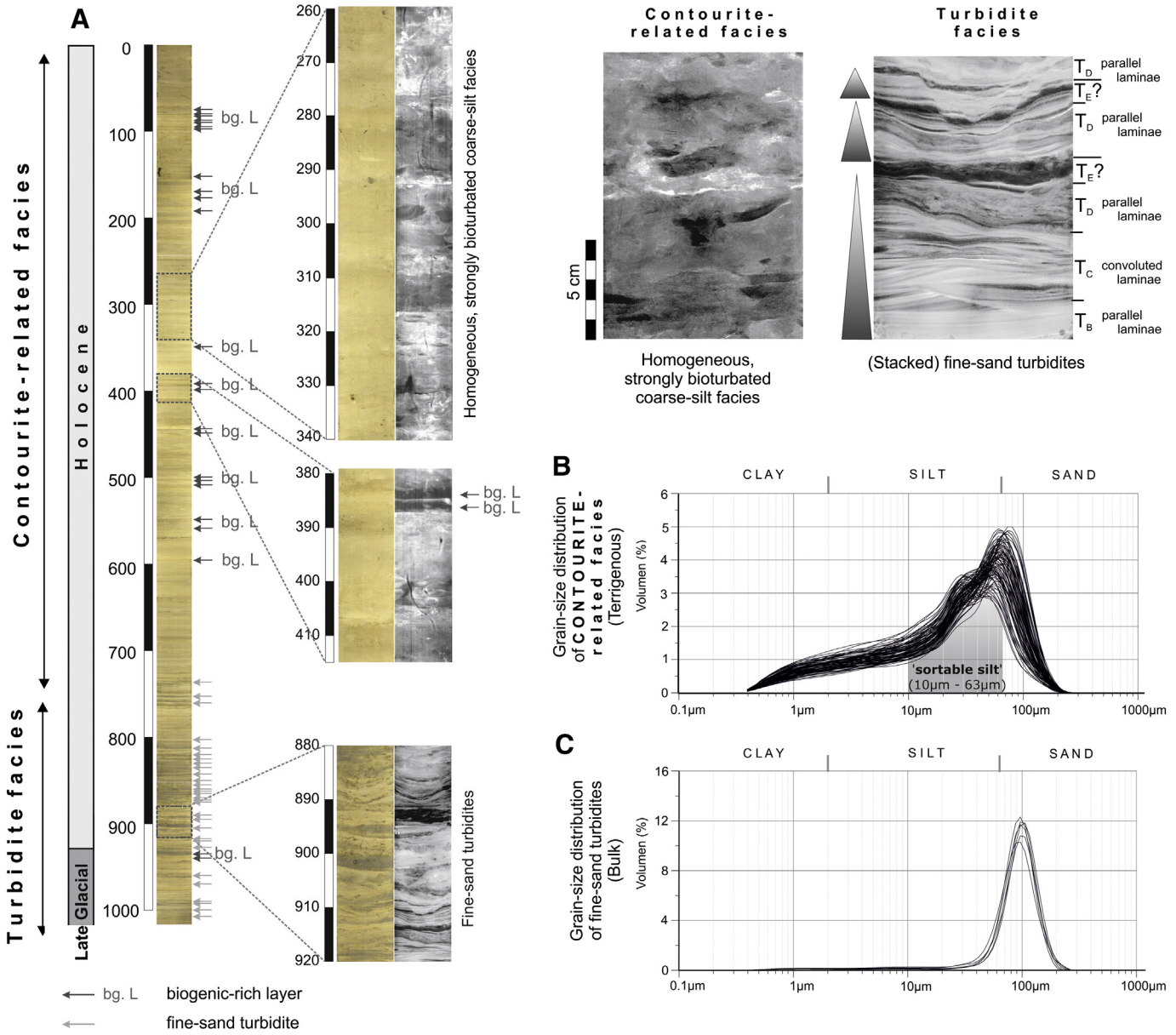

Fig. 4. (A) Line-scan images and X-radiographs of sediment core GeoB13862-1 reveal different sedimentary structures between the Holocene and the Late Glacial facies. The Holocene contourite-related facies is characterized by homogenous, strongly bioturbated coarse-silt sediments. This facies is intercalated at distinct intervals by biogenic-rich layers. In contrast, the Late Glacial turbidite facies is characterized by (partly) stacked fine-sand turbidites. (B) Terrigenous grain-size distribution of the Holocene contourite-related facies which is dominated by the "sortable silt" fraction (10–63 µm) (McCave et al., 1995). (C) Bulk grain-size distributions of Late Glacial fine-sand turbidites.

is the strong bioturbation present throughout all cores. The terrigenous fraction of the Holocene facies consist mainly of the "sortable silt" fraction (10–63 μm), i.e. the portion of the fine fraction whose particle size sorting responds directly to hydrodynamic processes (McCave et al., 1995; McCave, 2008) (Fig. 4B). The analysis of X-radiographs and the visual core descriptions indicate no turbidites in the Holocene sediments (Fig. 4). The only exception is GeoB13833-2 that shows a few mm-thin bedded, dark gray fine-sand turbidites intercalated at distinct intervals (Fig. 3).

4.1.2. Bulk components

The Holocene sedimentary sequence is in general characterized by carbonate-rich (~15%) and organic carbon-rich (~2.2%) sediments (Fig. 5). TOC concentrations of up to 2.2% indicate a preferred deposition of organic material in the Holocene, in particular between 8–5 and 3–1 ka B.P. (Fig. 5). Associated with these phases of generally enhanced accumulation of organic matter, the Holocene facies is intercalated by mm-thick layers enriched in biogenic opal (~15%) (Figs. 4, 5). These layers are composed of high percentages of marine phytoplankton (e.g., diatoms, silicoflagellates) and, consequently, mark prominent peaks in the Si/Al records (Fig. 5).

4.1.3. Grain-size distribution

Variations in the bulk grain-size distribution also appear to be related to the changes of TOC (Fig. 5). The additional influx of fine-grained material (10–20 μm) is associated to high TOC values, but is not observed in the terrigenous fraction which indicates a rather biogenic composition. The relative proportions of the sediment sub-fractions are similar in the sediment cores in which the coarse-silt fraction dominates the grain-size distribution during the Holocene (Fig. 5). GeoB13832-2 reveals average silt percentages of around 50%, while GeoB13833-2 and GeoB13862 are characterized by higher silt contents of around 70% which indicates a fining trend in grain-size toward the exit of the canyon. In all sediment cores the variability in silt and sand percentages shows a twofold pattern, and clay makes up a minor fraction with continuous percentages of up to 10%.

4.2. Transition Late Glacial to Holocene: Turbidite facies

4.2.1. Sedimentary structures and characteristics

The transition from Late Glacial to Holocene is indicated by a progressive change of the sedimentary facies characterized by intercalated thin-bedded, dark gray fine-sand turbidites (Figs. 3 & 4). Grain-size distribution and characteristics of the fine-sand turbidites are shown in Fig. 4C. The turbidites consist of purely terrigenous material and represent quartz-rich fining-upward sequences. The thin-bedded turbidites show incomplete or so-called bottom/top cut-out sequences (Bouma, 1962). The deposits between the turbidites do not indicate a (hemi) pelagic origin. They are similar to the Holocene sediments but reveal higher average sand percentages of ~40% (Fig. 5).

4.2.2. Bulk components

According to the bulk geochemical composition, the coarse-grained sediments between the turbidites are characterized by organic carbon-poor and (≤0.7%) carbonate-poor (≤3%) sediments (Fig. 5).

5. Discussion

5.1. Holocene

5.1.1. Contour-current controlled sedimentation in the Mar del Plata Canyon

The Mar del Plata Canyon does not have any obvious connection to the shelf or an onshore river system (e.g., La Plata River) (Krastel et al., 2011) from where sediment material could be delivered directly to the canyon by gravitational down-slope processes. Further, the Holocene deposits in the canyon indicate no systematic turbidite deposits. We thus can exclude a nearby direct source on the shelf and/or adjacent terrestrial environment for the sediments deposited in the canyon.

The presence of the Mar del Plata Canyon in a CDS instead suggests an influence of along-slope transport processes. The depocenter of the Holocene facies is located in the upper part of the Mar del Plata Canyon (Fig. 3), next to the Ewing terrace which is primarily affected by northward-flowing AAIW and UCDW (Hernández-Molina et al., 2009) (Fig. 2B). The remarkably high and continuous Holocene sedimentation rates in the canyon are coherent with sedimentation rates reported for drift deposits (Howe et al., 1994, 2002). Since contour currents are semi-permanent features in the ocean basins, they act almost continuously to affect sedimentation patterns. Therefore, we suggest that the rapidly accumulating and almost continuously deposited coarse-silt sediments in the Mar del Plata Canyon could be related to the activity of a near-bottom current.

The dominance of the "sortable silt" fraction over other particle sizes in the canyon cores also indicates a response to hydrodynamic processes (McCave et al., 1995; McCave, 2008) (Fig. 4B), and strongly supports the hypothesis of current-controlled sedimentation in the Mar del Plata Canyon. Small-scale primary sedimentary structures (e.g., parallel and/or cross-laminae, ripples, internal erosional surfaces) are lacking in our sediment cores due to bioturbation (Fig. 4). However, pervasive bioturbation itself could be an important diagnostic criterion for current-controlled sedimentation (Stow and Faugères, 2008; Wetzel et al., 2008). Because suspended organic matter is often adsorbed at the fine-grained material (Mayer, 1994), contour currents commonly supply food to deep-marine benthic organisms increasing their activity (Thistle et al., 1985; Lavaleye et al., 2002). In contrast to rapid sedimentary events such as turbidity current deposition, where the original structural sequences are often preserved, a pervasive bioturbation is an indicator for continuous sedimentation in the Mar del Plata Canyon. Accordingly, the sedimentary characteristics of the Holocene facies in the Mar del Plata Canyon indicate contourite-related sediment deposits (Fig. 4), and thus an influence of current-controlled sediment transport processes in the canyon.

Although the high sedimentation rates and grain-size characteristics of the Holocene deposits do not suggest (hemi) pelagic sedimentation as the major controlling sedimentary process, we have to consider that biogenic components (e.g., planktonic foraminifera) could be delivered by pelagic sedimentation from the overlying surface waters. In contrast to other sedimentary components, planktonic foraminifera settle rapidly from the overlying surface waters and are not easily re-distributed by bottom current activity (Fok-Pun and Komar, 1983; Ohkouchi et al., 2002), even not in the (high) energetic current regime of the Southwest Atlantic (Mollenhauer et al., 2006). Further, the intercalated biogenic-rich layers indicate an involvement of (hemi) pelagic sediments probably related to episodic productivity events of the upper water column during the Holocene (see Section 5.1.4).

5.1.2. Interaction of the Mar del Plata Canyon with the AAIW nepheloid layer

McCave (1986) has demonstrated that a clear relationship exists between regions of high deep-sea current velocity and the presence of nepheloid layers (i.e., layers with high suspended sediment load). Nepheloid layers can thus be useful indicators of strong current activity. Measurements of high turbidity south of the Mar del Plata Canyon suggest the presence of an intermediate nepheloid layer (INL) probably fed by erosive margin processes within the AAIW (Fig. 2A). Nepheloid layers at intermediate depths are well documented in various studies (e.g., McCave and Carter, 1997). Accordingly, unconsolidated sediments can be winnowed from the sea floor and become resuspended, transported and redeposited by the AAIW. Thereby, the grain size and amount of sediments within the nepheloid layer depend in general on the intensity of the deep-sea current (He et

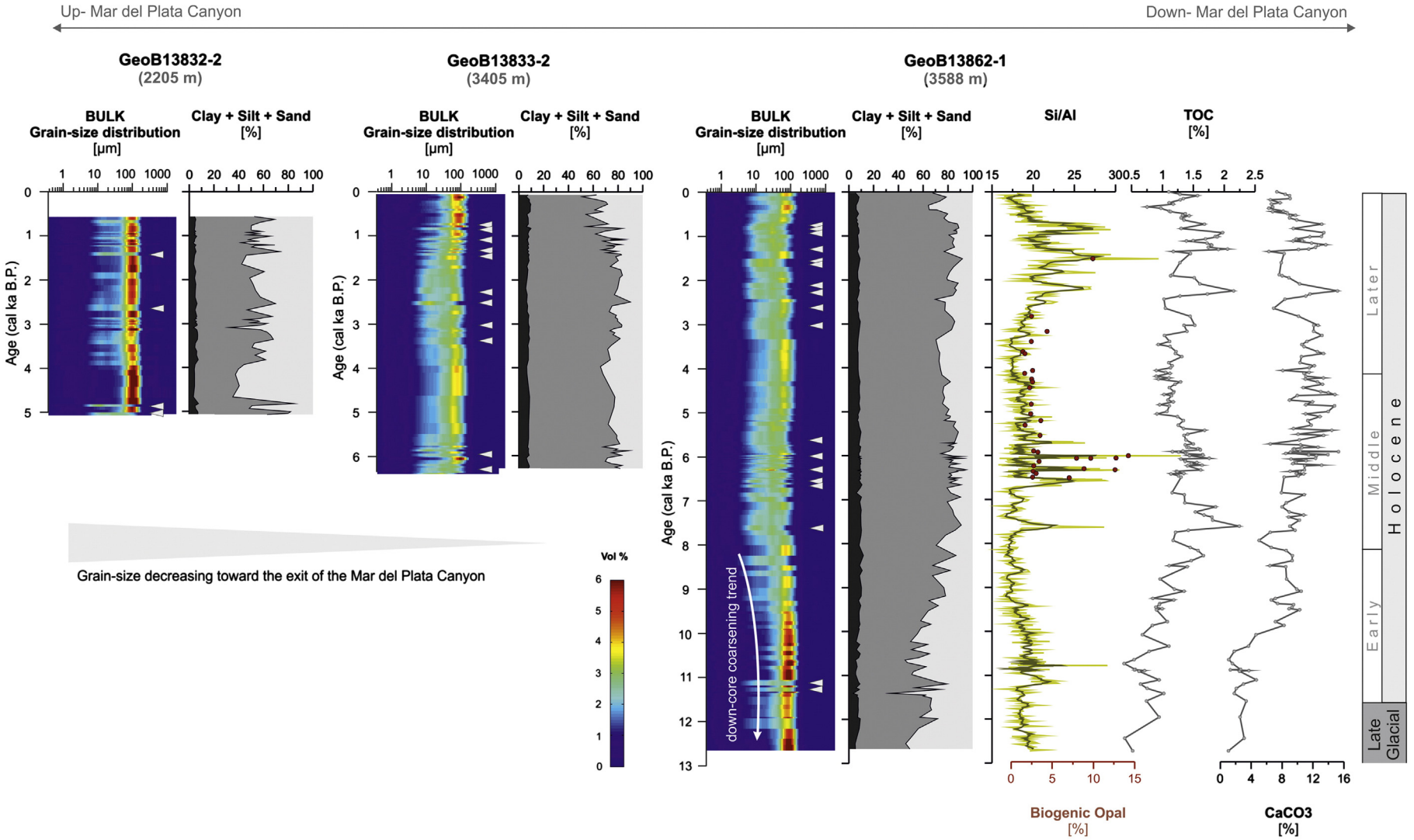

Fig. 5. Bulk grain-size distribution for sediment cores GeoB13832-2, GeoB13833-2 and GeoB13862-1 indicates a sediment-fining trend toward the exit of the Mar del Plata Canyon. Bulk grain-size distribution for GeoB13862-1 shows a down-core coarsening trend (Late Glacial turbidites not shown here). White triangles mark biogenic-rich layers. As shown for GeoB13862-1 these layers are reflected by prominent peaks in the Si/Al records.

al., 2008). The AAIW and more specifically its deepest portion associated with the nepheloid layer significantly influence the depositional pattern along the Ewing terrace (Preu et al., 2013). While the upper part of the Mar del Plata Canyon is directly located at the Ewing terrace, the sedimentation processes in the canyon might also be strongly affected by the INL (Fig. 2A, B). Hence, we propose that the Holocene sedimentary sequences were delivered to the Mar del Plata Canyon by the AAIW nepheloid layer which transported a considerable amount of sediments in suspension, and probably interacted with the canyon.

Preu et al. (2013) described a change in contourite drift construction around the Mar del Plata Canyon (Fig. 2B). Accordingly, drift deposits occur south of the canyon, but are not observed directly to the north of it. This change in depositional pattern around the Mar del Plata indicates a possible interaction of the canyon with the northward-flowing AAIW; which primarily influences drift deposition along the Ewing terrace. A change in depositional pattern around the canyon can also be interpreted by the differences of modern sediments at the Ewing terrace (Bozzano et al., 2011) (Fig. 2B). The sedimentological data thus indicate a lateral change in the energetic environment south of the canyon, showing a gradient from erosion processes in the contourite channel to deposition processes at the drift's crest (Fig. 2B). Accordingly, south of the canyon the water masses seem to be capable of winnowing and eroding the sea floor, thereby causing hiatuses and/or hardgrounds at the inner parts of the Ewing terrace; while deposition of sandy–silty contourites takes place at the outer parts of the Ewing terrace (Bozzano et al., 2011). In contrast to the presence of erosive and contourite depositional features south of the canyon, the modern sedimentation processes directly north of the canyon do not indicate such lateral change in depositional pattern, and instead are characterized by (hemi) pelagic sedimentation (Bozzano et al., 2011) (Fig. 2B). These changes in depositional pattern indicate a decrease of the flow energy between the southern and northern sides of the Mar del Plata Canyon. Thus, we propose that the canyon alters the circulation of the northward-flowing AAIW; in particular its deepest portion associated with the nepheloid layer which primarily influences the depositional pattern along the Ewing terrace (Preu et al., 2013).

The interaction of a deep-sea current with a submarine canyon has been described in the Gulf of Cadiz by Marchès et al. (2007). Marchès et al. (2007) suggest that a sharp change in the erosion/deposition pattern across the Portimão Canyon is due to the down-slope deviation of the Mediterranean Outflow Water. Along-slope salinity and dissolved oxygen sections from the vicinity of the Mar del Plata Canyon are presented in Fig. 6A, and B. Two of the hydrographic stations used to produce the section were located inside the canyon. The salinity and oxygen sections suggest horizontally stratified water masses around and within the canyon. A similar picture emerges from the CTD cast performed inside the canyon during R/V Meteor cruise M78/3a,b (Fig. 6C). In contrast to the situation described in Marchès et al. (2007), a horizontal stratification around and within the canyon does not indicate that the Mar del Plata Canyon captures the AAIW. Though the Mar del Plata Canyon appears to alter the circulation of AAIW, this water does not flow down the canyon simply because it is not dense enough to do so. In general, the flow over canyons of complex topography and the role of stratification in the associated circulation are poorly understood (e.g., Haidvogel and Beckman, 1995; Hickey, 1995). Theoretical considerations based on potential vorticity conservation arguments and numerical simulations indicate that the flow tends to follow the isobaths. The flow over a canyon will thus describe a cyclonic loop and will tend to accelerate slightly along the canyon walls (Klinck, 1996). Along the canyon axis, however, the simulated circulation tends to be weaker which may have a significant impact on the sedimentation processes at that location. As AAIW flows over the Mar del Plata Canyon the above described flow pattern may drastically decrease the transport capacity of the AAIW nepheloid layer. A decrease of the flow speed and transport capacity will thus cause sedimentation of the suspended load from the INL (Fig. 6C). Thereby, a considerable amount of sediments will be released

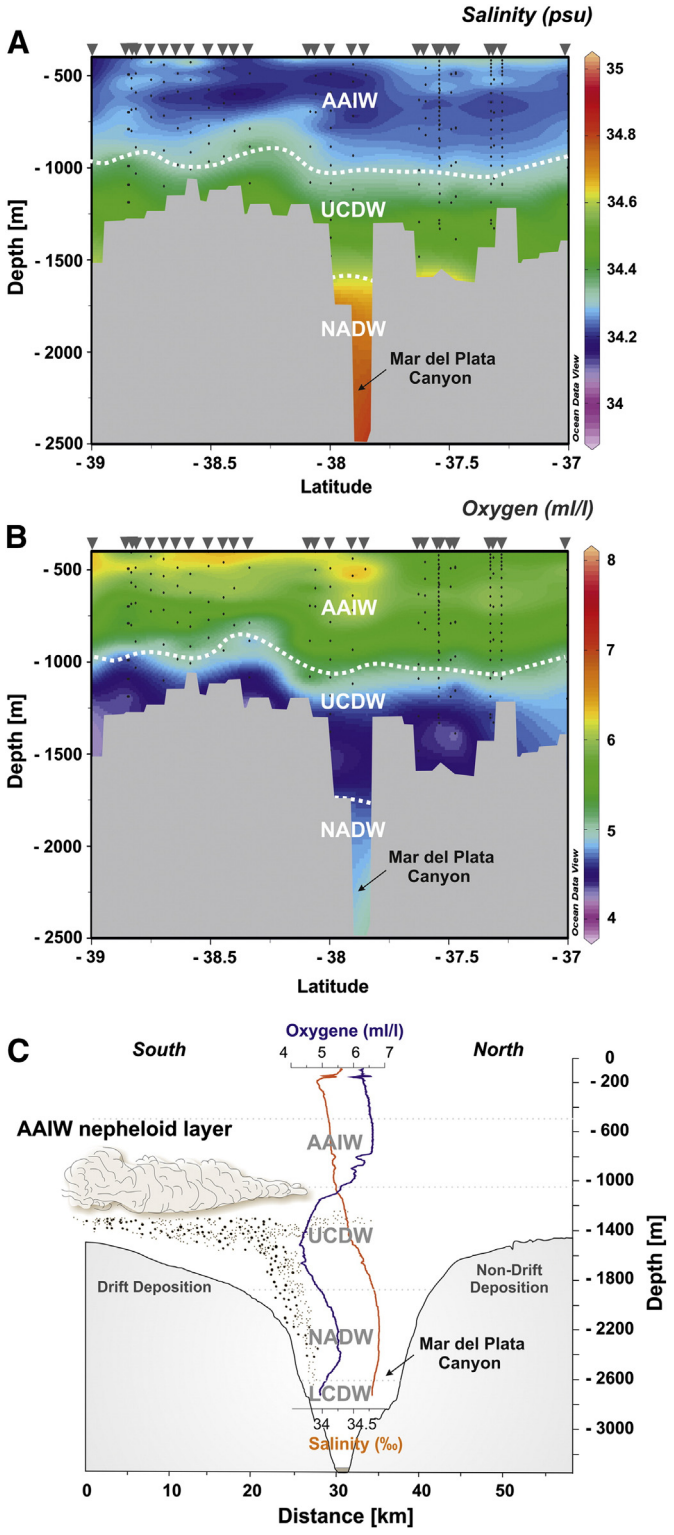

Fig. 6. (A + B) Along-slope salinity and dissolved oxygen section in the vicinity of the Mar del Plata Canyon show horizontal water column stratification within the canyon. (C) Schematic flow of the northward-flowing AAIW nepheloid layer over the Mar del Plata Canyon. By crossing the canyon the suspended material of the AAIW nepheloid layer is released into the canyon which causes remarkably high sedimentation rates. Oxygen (blue line) and salinity (orange line) depth profiles from CTD cast at the location of sediment core GeoB13833-2 indicate that the deeper portions of the canyon are clearly filled by NADW and LCDW. Accordingly, the AAIW is not captured by the canyon. AAIW — Antarctic Intermediate Water; UCDW — Upper Circumpolar Deep Water; NADW — North Atlantic Deep Water. (For interpretation of the references to color in this figure legend, the reader is referred to the web version of this article.)

into the Mar del Plata Canyon leading to the remarkably high and continuous sedimentation rates in the canyon. Thus, we assume that a change in hydrodynamic processes of AAIW is rather caused by 'crossing' the canyon, than by capturing and/or related down-canyon flowing of water masses as suggested by Marchès et al. (2007). However, a complete understanding of the near bottom flow and the sediment transport around the Mar del Plata Canyon will require direct observation of the flows, and thus our conclusion remains somewhat speculative.

5.1.3. Lateral differences in sedimentary pattern within the Mar del Plata Canyon

Differences in sedimentary pattern across the Ewing terrace result from the differences in the flow of AAIW and UCDW (Bozzano et al., 2011; Preu et al., 2013). We also observe differences in the sediment cores collected in the Mar del Plata Canyon with a decrease in sedimentation rates and a fining trend in grain-size toward the exit of the canyon (Figs. 3, 5). Accordingly, our shallowest core (GeoB13832-2) reveals a much higher content of fine-sand than the other sediment cores. This core is located directly in front of the inner part of the Ewing terrace where erosion/non-deposition takes place south of the Mar del Plata Canyon (Fig. 2B). We assume that associated with the strong erosion within the AAIW, the nepheloid layer is able to transport coarse-grained material, thereby being responsible for the deposition of sediments with this grain-size in the upper part of the canyon. The higher sedimentation rates from GeoB13832-2 could also be explained by the high current activity of the AAIW resulting in high suspended sediment load of the nepheloid layer.

In contrast, directly beneath the high velocity core of the AAIW, toward the interface of AAIW/UCDW, sediment material accumulates from the suspension of the nepheloid layer and leads to the formation of drift deposits on the Ewing terrace south of the Mar del Plata Canyon (Preu et al., 2013) (Fig. 2B). Through the gradual decrease of current velocities, the grain-size and the amount of suspended material within the INL decrease as well. Therefore, fine-grained material is delivered from the AAIW nepheloid layer into the canyon which would also explain the decrease in sedimentation rates down the canyon. Accordingly, GeoB13833-2 and GeoB13862-1 located in front of the outer parts of Ewing terrace reveal higher contents of fine-grained material (Fig. 5). However, our deepest sediment core (GeoB13861-1) shows a marked decrease in sedimentation rates (Fig. 3), which suggest that the lower parts of the canyon are not directly affected by the AAIW and UCDW activity.

5.1.4. The Mar del Plata Canyon as a climate archive

The biogenic-rich layers intercalated in the Holocene facies are enriched in biogenic opal (~15%) and, as a consequence, mark prominent peaks in the Si/Al records of all canyon cores (Fig. 7). They are

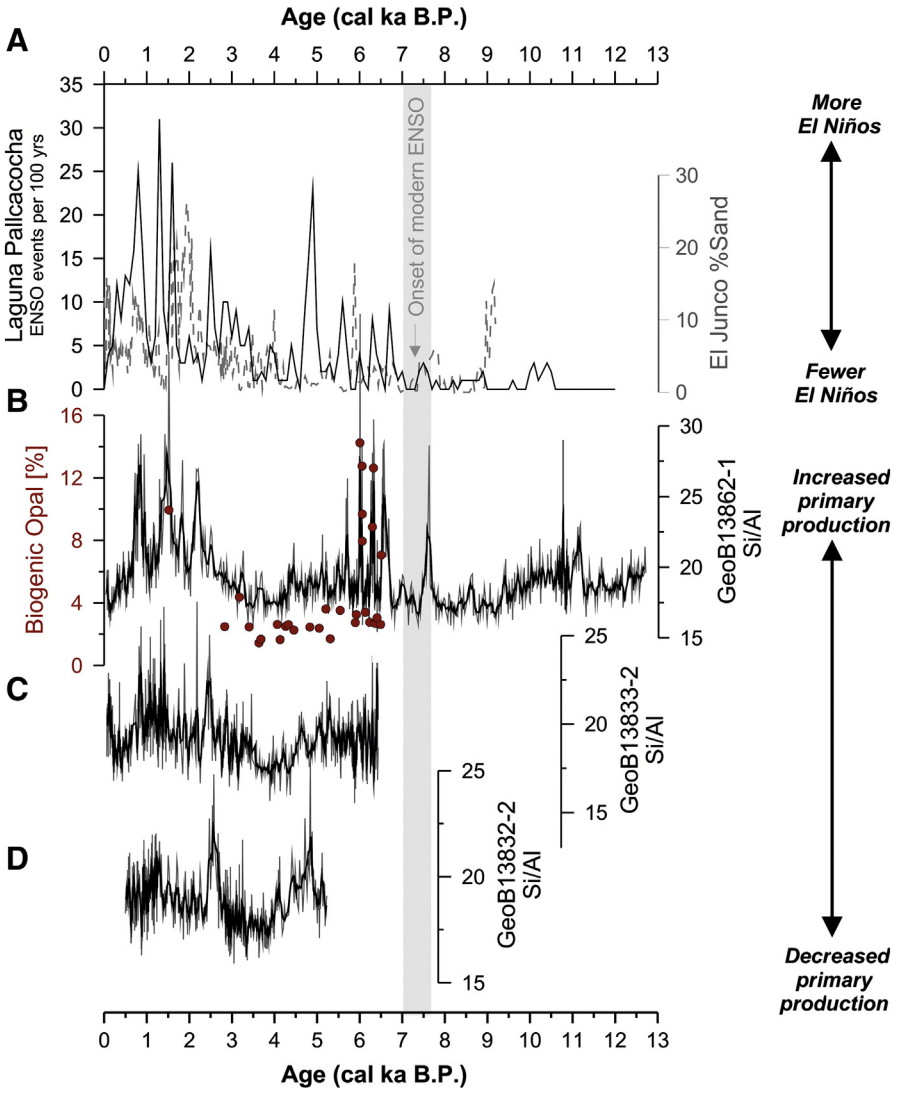

Fig. 7. (A) El Niño Southern Oscillation (ENSO) reconstructions from Laguna Pallcacocha (Moy et al., 2002) (black) and El Junco Lake (Conroy et al., 2008) (light gray dashed line). (B) Biogenic opal and Si/Al records of GeoB13862-2. (C) Si/Al record of GeoB13833-2. (D) Si/Al record of GeoB13832-2. Si/Al peaks indicate a high amount of biogenic opal and reflect anomalous positive productivity events in the upper water column above the Mar del Plata Canyon.

composed of high percentages of marine phytoplankton (e.g., diatoms, silicoflagellates) reflecting enhanced accumulation of pelagic sediments, presumably in response to increased productivity events in the upper water column above the Mar del Plata Canyon. Within age-model uncertainties the timing of these layers seems to be associated to the past variability of El Niño/Southern Oscillation (ENSO) (Moy et al., 2002; Conroy et al., 2008) (Fig. 7). Although the temporal resolution of the Mar del Plata Canyon cores is in general lower than the one needed to reconstruct individual ENSO events, the majority of biogenic-rich layers correlate to higher ENSO frequency and longer, stronger El Niño events. In particular the Si/Al record of GeoB13862-1 is significantly correlated with the ENSO index of Moy et al. (2002) ($r = 0.53$; $p < 0.01$).

There are two possible sources of variability in the primary production and particle flux in the Southwest Atlantic: one is associated with changes in the location of the Patagonian shelf break front (Romero et al., 2006) and the other with changes in the distribution of La Plata derived waters (Piola et al., 2000). Based on the foraminiferal oxygen isotopic analyses performed on samples from different sediment cores obtained in- and outside the Mar del Plata Canyon (not shown here), we suggest that changes of the Patagonian shelf break front are not correlated with the intercalated biogenic-rich layers. We therefore assume that changes in the distribution of La Plata derived waters set the pace of the observed layering in the Mar del Plata Canyon throughout the Holocene.

The La Plata plume is normally deflected northward along the continental shelf (Fig. 8A), fertilizing the Uruguayan and southern Brazilian shelf waters. Nevertheless, the northward plume dispersion is highly dependent on prevailing winds and undergoes large interannual variations related to ENSO (Piola et al., 2005, 2008). Accordingly, anomalously strong NE winds associated with El Niño events prevent an along-shore northward spreading of the La Plata plume and force the high-nutrient fluvial waters offshore (Piola et al., 2005, 2008) (Fig. 8B), which positively impact primary production and particle flux (Garcia and Garcia, 2008). Moreover, during El Niño events large precipitation anomalies occur over most of the La Plata drainage basin (Ropelewski and Halpert, 1987; Kiladis and Diaz, 1989), which significantly increases the discharge of the major La Plata tributaries (Mechoso and Iribarren, 1992; Depetris et al., 1996) (Fig. 8B). As the La Plata discharge influences the pelagic ecosystems by the injection of nutrients and increase in phytoplankton biomass (Ciotti et al., 1995), we assume that atmospheric circulation anomalies during high frequency and strong El Niño events fertilize the upper water column in the vicinity of the Mar del Plata Canyon by forcing the La Plata water masses offshore. The intercalated biogenic-rich layers in the canyon cores are thus probably related to a combination of conspicuously strong outflow events of the La Plata River and increased strength in NE winds over SE South America and the adjacent ocean, both associated to El Niño events.

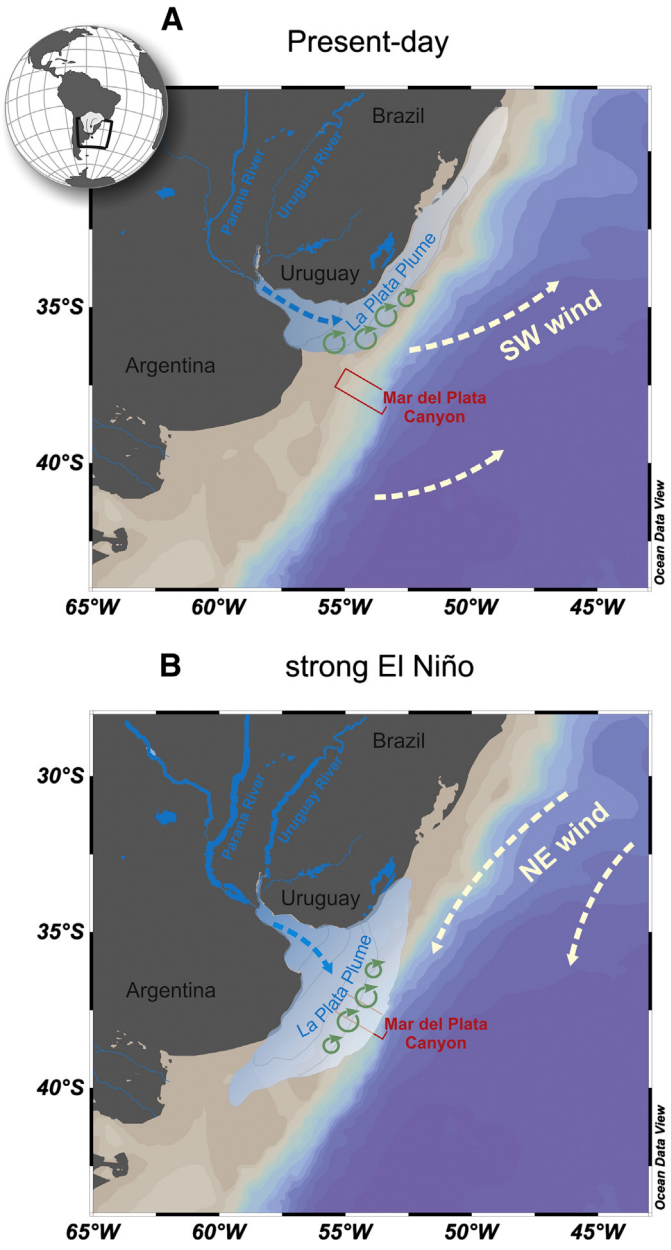

Fig. 8. Schematic outflow pattern of the La Plata River plume modified after Piola et al. (2005, 2008). (A) Present-day plume extension is directed northward along the Uruguayan and southern Brazilian shelf. (B) The combined effects of wind and precipitation anomalies during strong El Niño events in southeastern South America induce anomalously large outflow events of the La Plata River spreading offshore, thereby increasing phytoplankton biomass and production in the upper water column above the Mar del Plata Canyon.

5.2. Transition Late Glacial/Holocene

5.2.1. Current-controlled turbidite deposition in the Mar del Plata Canyon

Gravitational processes dominate the depositional pattern in the Mar del Plata Canyon during the transition Late Glacial/Holocene. As already discussed the Mar del Plata Canyon does not have any obvious connection to the La Plata River (Krastel et al., 2011) from where sediment could be delivered directly by gravitational down-slope processes.

Rivers that enter the ocean can generate surface (hyperpycnal) plumes which descend to the sea floor as a result of the excess density generated by its sediment load (Parsons et al., 2001; Mulder et al., 2003; Ducassou et al., 2008). Hyperpycnal plumes are a class of sediment-laden gravity current; they are recognizable by their deposits, commonly referred as fine-grained turbidites (i.e., muddy turbidites). Accordingly, the coarse-grained type of turbidites in the Mar del Plata Canyon does not support that kind of process. Further, submarine channels indicate that the La Plata River extended northwards over the exposed continental shelf during the last glacial (Ewing and Lonardi, 1971). Chiessi et al. (2008) showed that the huge sedimentary load of the La Plata River was directly delivered to the Rio Grande Cone, a major sedimentary feature in the western Argentine Basin located to the north of the Mar del Plata Canyon. We therefore do not consider the La Plata River as a major source for the intensified turbidite formation in the Mar del Plata Canyon.

The turbidites in the canyon reflect the same lithological characteristics as the drift deposits at the outer Ewing terrace which consist of dark gray, fine-sand with a siliciclastic composition (Bozzano et al., 2011). We therefore assume that turbidity-current activity during the transition Late Glacial/Holocene may be related to sediment instability of drift deposits at the southern flank of the canyon. Recent studies

suggest that the formation and northward penetration of Antarctic water masses were enhanced during the last glacial termination (e.g., Pahnke et al., 2008; Hendry et al., 2012). Related to the change in flow strength and associated increase of accumulation of sediments, the plastered drift deposits on the outer part of the Ewing terrace were probably growing during that period. Hence, a down-current migration/progradation of drift deposits would be possible (Mulder et al., 2006) and would lead to local instability near the southern flank of the canyon which in turn results in gravitational processes like turbidity-currents. This assumption is also supported by a general coarsening of the current-controlled sedimentation in the canyon during the transition phase indicating a general increase in the strength of AAIW (Fig. 5). A general decrease in current speed of the Antarctic water masses during the Holocene (Pahnke et al., 2008) would not promote progradation of the drift deposits. Accordingly, the Holocene facies does not show any down-canyon transport processes, except for GeoB13833-2 which is located directly in front of the drift deposits on the Ewing terrace, and therefore preferably affected by instability events of the drift deposits.

6. Conclusion

The Mar del Plata Canyon is located at the continental margin off northern Argentina and intersects a CDS that is formed by the northward-flowing Antarctic water masses (i.e., AAIW and UCDW). The canyon interacts with the intermediate nepheloid layer of the AAIW which results in rapid and continuous deposition of coarse-silt material (i.e., "sortable silt", 10–63 μm) in the canyon with remarkably high sedimentation rates of around 160 cm/kyr during the Holocene. The deposits inside the canyon reveal sediment characteristics similar to drift deposits and are characterized by strongly bioturbated coarse-silt sediments without primary structures. The sedimentary pattern in the canyon indicates a response to changes of contour-current strength of AAIW most probably related to climate variability. Accordingly, we interpret stronger (weaker) circulation of the AAIW during the Late Glacial (Holocene). The influence of (lateral) current-controlled transport processes on the sedimentation pattern in a submarine canyon appears to be an important process at continental margins which are affected by deep-water current activity. In highly energetic current regions as the Southwest Atlantic, where contour currents rework significant amounts of sediment, a submarine canyon can act as a sink for enhanced accumulation of sediments, thereby holding a great potential as a climate archive. Accordingly, the Mar del Plata Canyon recorded anomalously positive productivity events in the water column over the canyon that were correlated with periods of strong El Niño activity during the Holocene. Large positive precipitation anomalies over SE South America associated with El Niño events significantly increased the discharge of the La Plata River that in turn enhanced the primary production. Due to atmospheric circulation and precipitation anomalies the La Plata plume spread offshore, leading to event-like accumulation of biogenic-rich layers in the Mar del Plata Canyon.

Acknowledgments

We thank the two Reviewers and the Editor for their thorough and constructive comments that improved the manuscript. We also thank B. Kockisch and M. Klann for their lab work (MARUM, Bremen), and K.H. Baumann and G. Fischer for comments and discussion. We acknowledge the help of Inka Meyer for guidance during grain-size analyses. We thank Dr. Ursula Röhl and her team for assistance during XRF scanning. This study was funded through the DFG-Research Center/Cluster of Excellence "The Ocean in the Earth System" and was supported by GLOMAR – Bremen International Graduate School for Marine Sciences. ARP acknowledges the support from grant CRN2076 from the Inter-American Institute for Global Change Research and the U.S. National Science Foundation grant GEO-0452325. CMC acknowledges the support from FAPESP (2010/09983-9, 2012/17517-3). Further, we thank the members of the shipboard and scientific crews of the RV Meteor cruise M78/3a,b. The data of this study are available in the PANGAE database.

References

Bouma, A.H., 1962. Sedimentology of Some Flysch Deposits: Graphic Approach to Facies Interpretation. Elsevier, Amsterdam 168.
Bozzano, G., Violante, R., Cerredo, M., 2011. Middle slope contourite deposits and associated sedimentary facies off NE Argentina. Geo-Marine Letters 31 (5), 495–507.
Carreto, J., Lutz, V.A., Carignan, M.O., Cucchi Colleoni, A.D., De Marco, S.G., 1995. Hydrography and chlorophyll a in a transect from the coast to the shelf-break in the Argentinian Sea. Continental Shelf Research 15 (2–3), 315–336.
Carson, B., Baker, E.T., Hickey, B.M., Nittrouer, C.A., DeMaster, D.J., Thorbjarnarson, K.W., Snyder, G.W., 1986. Modern sediment dispersal and accumulation in Quinault submarine canyon — a summary. Marine Geology 71 (1–2), 1–13.
Chelton, D.B., Schlax, M.B., Witter, D.L., Richman, J.G., 1990. Geosat altimeter observations of the surface circulation of the Southern Ocean. Journal of Geophysical Research 95 (C10), 17, 877–17, 903.
Chiessi, C.M., Mulitza, S., Paul, A., Pätzold, J., Groeneveld, J., Wefer, G., 2008. South Atlantic interocean exchange as the trigger for the Bølling warm event. Geology 36 (12), 919–922.
Ciotti, Á.M., Odebrecht, C., Fillmann, G., Moller Jr., O.O., 1995. Freshwater outflow and Subtropical Convergence influence on phytoplankton biomass on the southern Brazilian continental shelf. Continental Shelf Research 15 (14), 1737–1756.
Conroy, J.L., Overpeck, J.T., Cole, J.E., Shanahan, T.M., Steinitz-Kannan, M., 2008. Holocene changes in eastern tropical Pacific climate inferred from a Galápagos lake sediment record. Quaternary Science Reviews 27 (11–12), 1166–1180.
DeMaster, D.J., 1981. The supply and accumulation of silica in the marine environment. Geochimica et Cosmochimica Acta 45 (10), 1715–1732.
Depetris, P.J., Kempe, S., Latif, M., Mook, W.G., 1996. ENSO-controlled flooding in the Paraná River (1904–1991). Naturwissenschaften 83 (3), 127–129.
Ducassou, E., Mulder, T., Migeon, S., Gonthier, E., Murat, A., Revel, M., Capotondi, L., Bernasconi, S.M., Mascle, J., Zaragosi, S., 2008. Nile floods recorded in deep Mediterranean sediments. Quaternary Research 70 (3), 382–391.
Ewing, M., Lonardi, A.G., 1971. Sediment transport and distribution in the Argentine Basin. 5. Sedimentary structure of the Argentine margin, basin and related provinces. In: Ahrens, L.H., Press, F., Runcorn, S.K., Urey, H.C. (Eds.), Physics and Chemistry of the Earth, vol. 8. Pergamon, Oxford, pp. 123–251.
Fok-Pun, L., Komar, P.D., 1983. Settling velocities of planktonic foraminifera; density variations and shape effects. Journal of Foraminiferal Research 13 (1), 60–68.
Garcia, C.A.E., Garcia, V.M.T., 2008. Variability of chlorophyll-a from ocean color images in the La Plata continental shelf region. Continental Shelf Research 28 (13), 1568–1578.
Govin, A., Holzwarth, U., Heslop, D., Ford Keeling, L., Zabel, M., Mulitza, S., Collins, J.A., Chiessi, C.M., 2012. Distribution of major elements in Atlantic surface sediments (36°N–49°S): imprint of terrigenous input and continental weathering. Geochemistry, Geophysics, Geosystems 13, Q01013.
Gwilliam, C.S., 1996. Modelling the global ocean circulation on the T3D. In: Ecer, A., Periaux, J., Satdfuka, N., S. TaylorA2, S., Ecer, A., J.P.N.S., Taylor, S. (Eds.), Parallel Computational Fluid Dynamics 1995. North-Holland, Amsterdam, pp. 33–40.
Haidvogel, D.B., Beckman, A., 1995. Wind-driven residual currents over a coastal canyon. In: Müller, P., Henderson, D. (Eds.), Proc. Hawaiian Winter Workshop on Topographic Effects in the Ocean. School of Ocean and Earth Science and Technology, University of Hawaii, Honolulu, pp. 219–224.
Harris, P.T., Whiteway, T., 2011. Global distribution of large submarine canyons: geomorphic differences between active and passive continental margins. Marine Geology 285 (1–4), 69–86.
He, Y., Duan, T., Gao, Z., 2008. Chapter 7 Sediment Entrainment. In: Rebesco, M., Camerlenghi, A. (Eds.), Developments in Sedimentology. Elsevier, pp. 99–119.
Hendry, K.R., Robinson, L.F., Meredith, M.P., Mulitza, S., Chiessi, C.M., Arz, H., 2012. Abrupt changes in high-latitude nutrient supply to the Atlantic during the last glacial cycle. Geology 40 (2), 123–126.
Hernández-Molina, F.J., Paterlini, M., Violante, R., Marshall, P., de Isasi, M., Somoza, L., Rebesco, M., 2009. Contourite depositional system on the Argentine Slope: an exceptional record of the influence of Antarctic water masses. Geology 37 (6), 507–510.
Hernández-Molina, F.J., Paterlini, M., Somoza, L., Violante, R., Arecco, M.A., de Isasi, M., Rebesco, M., Uenzelmann-Neben, G., Neben, S., Marshall, P., 2010. Giant mounded drifts in the Argentine Continental Margin: origins, and global implications for the history of thermohaline circulation. Marine and Petroleum Geology 27 (7), 1508–1530.
Hickey, B., 1995. Coastal submarine canyons. In: Müller, P., Henderson, D. (Eds.), Proc. Hawaiian Winter Workshop on Topographic Effects in the Ocean. School of Ocean and Earth Science and Technology, Univ. of Hawaii, Honolulu, pp. 95–110.
Howe, J.A., Stoker, M.S., Stow, D.A.V., 1994. Late Cenozoic sediment drift complex, northeast Rockall Trough, North Atlantic. Paleoceanography 9 (6), 989–999.
Howe, J.A., Stoker, M.S., Stow, D.A.V., Akhurst, M.C., 2002. Sediment drifts and contourite sedimentation in the northeastern Rockall Trough and Faroe-Shetland Channel, North Atlantic Ocean. Geological Society, London, Memoirs 22 (1), 65–72.
Hubold, G., 1980. Hydrography and plankton off southern Brazil and Rio de la Plata, spring cruise: August–November 1978. Atlantica 4, 1–22.
Hubold, G., 1980. Second report on hydrography and plankton off southern Brazil and Rio de la Plata, autumn cruise: April–June 1978. Atlantica 4, 23–42.
Jansen, J.H.F., Van der Gaast, S.J., Koster, B., Vaars, A.J., 1998. CORTEX, a shipboard XRF-scanner for element analyses in split sediment cores. Marine Geology 151 (1–4), 143–153.

Kiladis, G.N., Diaz, H.F., 1989. Global climatic anomalies associated with extremes in the Southern Oscillation. Journal of Climate 2 (9), 1069–1090.
Klinck, J.M., 1996. Circulation near submarine canyons: a modeling study. Journal of Geophysical Research 101 (C1), 1211–1223.
Krastel, S., Wefer, G., 2012. Report and preliminary results of RV METEOR Cruise M78/3. Sediment Transport off Uruguay and Argentina: From the Shelf to the Deep Sea; 19.05.2009–06.07.2009, Montevideo (Uruguay)–Montevideo (Uruguay) Berichte aus dem Fachbereich Geowissenschaften 285 (Fachbereich Geowissenschaften, Bremen).
Krastel, S., Wefer, G., Hanebuth, T., Antobreh, A., Freudenthal, T., Preu, B., Schwenk, T., Strasser, M., Violante, R., Winkelmann, D., party, M.s.s, 2011. Sediment dynamics and geohazards off Uruguay and the de la Plata River region (northern Argentina and Uruguay). Geo-Marine Letters 31 (4), 271–283.
Lastras, G., Acosta, J., Muñoz, A., Canals, M., 2011. Submarine canyon formation and evolution in the Argentine Continental Margin between 44°30′S and 48°S. Geomorphology 128 (3–4), 116–136.
Lavaleye, M.S.S., Duineveld, G.C.A., Berghuis, E.M., Kok, A., Witbaard, R., 2002. A comparison between the megafauna communities on the N.W. Iberian and Celtic continental margins — effects of coastal upwelling? Progress in Oceanography 52 (2–4), 459–476.
Marchès, E., Mulder, T., Cremer, M., Bonnel, C., Hanquiez, V., Gonthier, E., Lecroart, P., 2007. Contourite drift construction influenced by capture of Mediterranean Outflow Water deep-sea current by the Portimão submarine canyon (Gulf of Cadiz, South Portugal). Marine Geology 242 (4), 247–260.
Mayer, L.M., 1994. Surface area control of organic carbon accumulation in continental shelf sediments. Geochimica et Cosmochimica Acta 58 (4), 1271–1284.
McCave, I.N., 1986. Local and global aspects of the bottom nepheloid layers in the world ocean. Netherlands Journal of Sea Research 20 (2–3), 167–181.
McCave, I.N., 2008. Chapter 8 Size sorting during transport and deposition of fine sediments: sortable silt and flow speed. In: Rebesco, M., Camerlenghi, A. (Eds.), Developments in Sedimentology. Elsevier, pp. 121–142.
McCave, I.N., Carter, L., 1997. Recent sedimentation beneath the Deep Western Boundary Current off northern New Zealand. Deep Sea Research Part I: Oceanographic Research Papers 44 (7), 1203–1237.
McCave, I.N., Manighetti, B., Robinson, S.G., 1995. Sortable silt and fine sediment size/composition slicing: parameters for palaeocurrent speed and palaeoceanography. Paleoceanography 10 (3), 593–610.
Mechoso, C.R., Iribarren, G.P., 1992. Streamflow in Southeastern South America and the Southern Oscillation. Journal of Climate 5 (12), 1535–1539.
Mechoso, C.R., Dias, P.S., Baethgen, W., Barros, V., Berbery, E.H., Clarke, R., Cullen, H., Ereño, C., Grassi, B., Lettenmaier, D., 2001. Climatology and hydrology of the Plata Basin, a document of VAMOS Scientific Study Group on the Plata Basin. Available at http://www.clivar.org/science/vamos_pubs.htm.
Mollenhauer, G., McManus, J.F., Benthien, A., Müller, P.J., Eglinton, T.I., 2006. Rapid lateral particle transport in the Argentine Basin: molecular 14C and 230Thxs evidence. Deep Sea Research Part I: Oceanographic Research Papers 53 (7), 1224–1243.
Moy, C.M., Seltzer, G.O., Rodbell, D.T., Anderson, D.M., 2002. Variability of El Nino/Southern Oscillation activity at millennial timescales during the Holocene epoch. Nature 420 (6912), 162–165.
Mulder, T., Syvitski, J.P.M., Migeon, S., Faugères, J.-C., Savoye, B., 2003. Marine hyperpycnal flows: initiation, behavior and related deposits. A review. Marine and Petroleum Geology 20 (6–8), 861–882.
Mulder, T., Lecroart, P., Hanquiez, V., Marchés, E., Gonthier, E., Guedes, J.C., Thiébot, E., Jaaidi, B., Kenyon, N., Voisset, M., Perez, C., Sayago, M., Fuchey, Y., Bujan, S., 2006. The western part of the Gulf of Cadiz: contour currents and turbidity currents interactions. Geo-Marine Letters 26 (1), 31–41.
Mulitza, S., Prange, M., Stuut, J.-B., Zabel, M., von Dobeneck, T., Itambi, A.C., Nizou, J., Schulz, M., Wefer, G., 2008. Sahel megadroughts triggered by glacial slowdowns of Atlantic meridional overturning. Paleoceanography 23 (4), PA4206.
Müller, P.J., Schneider, R., 1993. An automated leaching method for the determination of opal in sediments and particulate matter. Deep Sea Research Part I: Oceanographic Research Papers 40 (3), 425–444.
Ohkouchi, N., Eglinton, T.I., Keigwin, L.D., Hayes, J.M., 2002. Spatial and temporal offsets between proxy records in a sediment drift. Science 298 (5596), 1224–1227.
Pahnke, K., Goldstein, S.L., Hemming, S.R., 2008. Abrupt changes in Antarctic Intermediate Water circulation over the past 25,000 years. Nature Geoscience 1 (12), 870–874.
Parsons, J.D., Bush, J.W.M., Syvitski, J.P.M., 2001. Hyperpycnal plume formation from riverine outflows with small sediment concentrations. Sedimentology 48 (2), 465–478.
Peterson, R.G., Stramma, L., 1991. Upper-level circulation in the South Atlantic Ocean. Progress in Oceanography 26 (1), 1–73.
Piola, A.R., Matano, R.P., 2001. Brazil And Falklands (Malvinas) Currents. In: John, H.S. (Ed.), Encyclopedia of Ocean Sciences. Academic Press, Oxford, pp. 340–349.
Piola, A.R., Campos, E.J.D., Möller Jr., O.O., Charo, M., Martinez, C., 2000. Subtropical Shelf Front off eastern South America. Journal of Geophysical Research 105 (C3), 6565–6578.
Piola, A.R., Matano, R.P., Palma, E.D., Möller Jr., O.O., Campos, E.J.D., 2005. The influence of the Plata River discharge on the western South Atlantic shelf. Geophysical Research Letters 32 (1), L01603.
Piola, A.R., Romero, S.I., Zajaczkovski, U., 2008. Space–time variability of the Plata plume inferred from ocean color. Continental Shelf Research 28 (13), 1556–1567.
Preu, B., Hernández-Molina, F.J., Violante, R., Piola, A.R., Paterlini, C.M., Schwenk, T., Voigt, I., Krastel, S., Spiess, V., 2013. Morphosedimentary and hydrographic features of the northern Argentine margin: the interplay between erosive, depositional and gravitational processes and its conceptual implications. Deep Sea Research Part I: Oceanographic Research Papers 75 (0), 157–174.
Rebesco, M., Camerlenghi, A., Van Loon, A.J., 2008. Chapter 1 contourite research: a field in full development. In: Rebesco, M., Camerlenghi, A. (Eds.), Developments in Sedimentology. Elsevier, pp. 1–10.
Reid, J.L., Patzert, W.C., 1977. On the characteristics and circulation of the Southwestern Atlantic Ocean. Journal of Physical Oceanography 7 (1), 62–91.
Reimer, P.J., Baillie, M.G.L., Bard, E., Bayliss, A., Beck, J.W., Blackwell, P.G., Bronk Ramsey, C., Buck, C.E., Burr, G.S., Edwards, R.L., Friedrich, M., Grootes, P.M., Guilderson, T.P., Hajdas, I., Heaton, T.J., Hogg, A.G., Hughen, K.A., Kaiser, K.F., Kromer, B., McCormac, F.G., Manning, S.W., Reimer, R.W., Richards, D.A., Southon, J.R., Talamo, S., Turney, C.S.M., van der Plicht, J., Weyhenmeyer, C.E., 2009. IntCal09 and Marine09 radiocarbon age calibration curves, 0–50,000 years cal BP. Radiocarbon 51, 1111–1150.
Romero, S.I., Piola, A.R., Charo, M., Garcia, C.A.E., 2006. Chlorophyll-a variability off Patagonia based on SeaWiFS data. Journal of Geophysical Research 111 (C5), C05021.
Ropelewski, C.F., Halpert, M.S., 1987. Global and regional scale precipitation patterns associated with the El Niño/Southern Oscillation. Monthly Weather Review 115 (8), 1606–1626.
Stow, D.A.V., Faugères, J.C., 2008. Chapter 13 contourite facies and the facies model. In: Rebesco, M., Camerlenghi, A. (Eds.), Developments in Sedimentology. Elsevier, pp. 223–256.
Stow, D.A.V., Lovell, J.P.B., 1979. Contourites: their recognition in modern and ancient sediments. Earth-Science Reviews 14 (3), 251–291.
Stow, D.A.V., Faugères, J.-C., Howe, J.A., Pudsey, C.J., Viana, A.R., 2002. Bottom currents, contourites and deep-sea sediment drifts: current state-of-the-art. Geological Society, London, Memoirs 22 (1), 7–20.
Stow, D.A.V., Hunter, S., Wilkinson, D., Hernández-Molina, F.J., 2008. Chapter 9 the nature of contourite deposition. In: Rebesco, M., Camerlenghi, A. (Eds.), Developments in Sedimentology. Elsevier, pp. 143–156.
Stramma, L., England, M., 1999. On the water masses and mean circulation of the South Atlantic Ocean. Journal of Geophysical Research 104 (C9), 20863–20883.
Stuiver, M., Reimer, P.J., 1993. Extended 14C data base and revised CALIB 3.0 14C age calibration program. Radiocarbon 35, 215–230.
Thistle, D., Yingst, J.Y., Fauchald, K., 1985. A deep-sea benthic community exposed to strong near-bottom currents on the Scotian Rise (western Atlantic). Marine Geology 66 (1–4), 91–112.
Urien, C.M., Ewing, M., 1974. Recent sediments and environment of Southern Brazil, Uruguay, Buenos Aires and Rio Negro continental shelf. In: Burk, C.A., Drake, C. (Eds.), Geology of Continental Margins. Springer-Verlag, Berlin.
Wetzel, A., Werner, F., Stow, D.A.V., 2008. Chapter 11 bioturbation and biogenic sedimentary structures in contourites. In: Rebesco, M., Camerlenghi, A. (Eds.), Developments in Sedimentology. Elsevier, pp. 183–202.